Ray tracing simulation of short wigglers for ESRF-EBS

M. Sanchez del Rio

April 20, 2016

1 Introduction

This document compares the radiation emission by different options for short insertion devices (ID) to be placed at the ports where bending magnet beamlines are installed.

Three important issues are adressed: the influence of the electron beam emittance, the aberrations played by a real focusing mirror and the effect of the overlapping radiation by the bending magnets near to the short IDs.

2 Configurations and parameters

The emission of different short insertion devices to be placed at the bending magnet ports is analyzed. They are also compared with the ESRF BM ($B = 0.856\,T$, current lattice). The effect of focusing is studied in three cases (summarized in Table 2): An ideal 1:1 focusing element (using an aberration-free optics, in our case an ellipsoid at $\theta = 45\ deg$ incidence), a 1:1 focusing toroidal mirror (for this configuration the aberrations of the toroidal mirror are negligeable as compared with the ellipsoid), and a 3:1 focusing ellipsoidal mirror (here an ellipsoid is important to supress most aberrations). No slope errors are considered (in fact, slope errors would promarly affect the tangential V direction, and the effects in the H sagittal direction which is more interesting for us are much less important). Ideal 100% reflectivity of the mirror is supposed in all cases (althogh it is certainly irrealistic for high photon energies, it permits to better study the effect of the sources).

Table 1: List and parameters of the focusing elements.

Name	Ratio	p	q	length	Grazing angle	Magnification
		m	m	m		
Ideal	1:1	30	30	∞	45 deg	1
Toroid	1:1	30	30	1	3 mrad	1
Ellipsoid	3:1	45	15	1	3 mrad	1/3

Three possible solutions for short ID to be placed at the BM ports are envisaged: a three pole wiggler (3P), a two pole wiggler in two configurations

(2PA and 2PB) and a super bending, bending magnet or one pole wiggler (1P). For comparison purposed, simulations are also given for the ESRF-I bending magnet (BM).

Fig. 2 shows the magnetic field produced by the magnets of these devices: Fig. 2a includes part of the magnetic field of the BM next to the ID. This is important, as the emission of these BM can superpose the emission of the IDs; Fig. 2b contains the same data as Fig. 1a but cut in the interval $-0.7 \leq s \leq 0.7$. This is used to study the isolated emission of the IDs.

For all calculations, nominal electron energy is $E = 6\ GeV$ and the electron current $I = 200\ mA$.

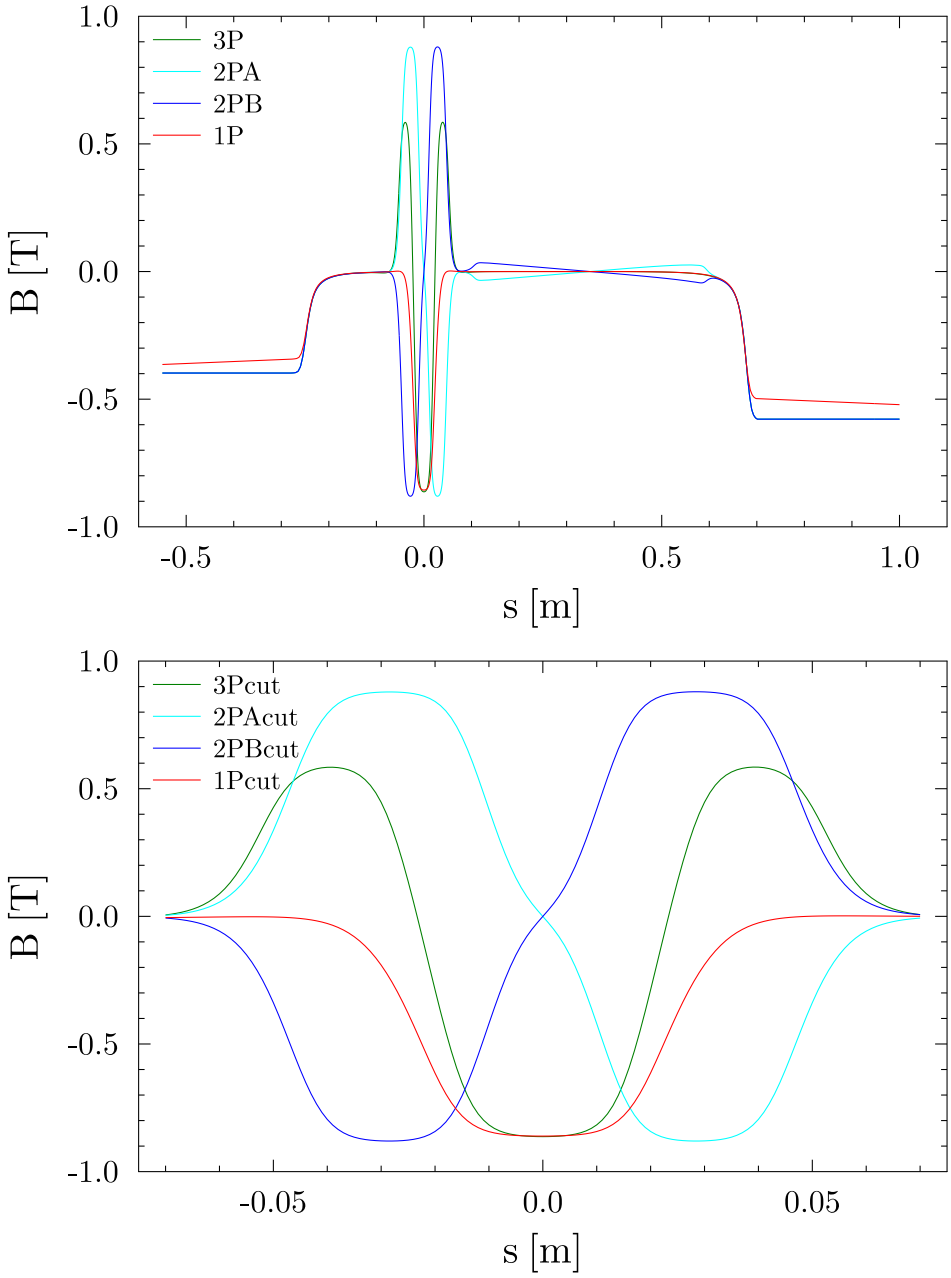

Figure 1: a) (Top) Magnetic field for the different short ID (data from Joel Chavanne). b) (Bottom) The same field data "cut" in a limited s interval only showing the field produced by the short ID's.

3 Radiation spectrum

The full emission spectrum produced by the IDs with magnetic field in Fig. 2b is compared with a the 0.856 T bending magnet (integrated over 2 $mrad$ horizontal divergence) in Fig. 3. It can be shown that the 1P spectrum is very similar to the current BM spectrum (over 2 $mrad$ horizontal divergence), The 2P is the most favorable case (both A and B configurations present the same emission spectrum because full emission is considered and magnetic field is the same except for a sign). The 3P is more intense than the BM at low photon energies, and practically the same at high energies. Table 3 contains flux values for the photon energies studied here.

Table 2: Some values of flux.

Device	5 keV	10 keV	20 keV	40 keV	80 keV
3P	7.81e+13	6.65e+13	4.22e+13	1.56e+13	2.14e+12
2PA	8.68e+13	7.8e+13	5.47e+13	2.37e+13	3.98e+12
2PB	8.68e+13	7.81e+13	5.47e+13	2.37e+13	3.99e+12
1P	5.39e+13	4.84e+13	3.37e+13	1.44e+13	2.33e+12
BM	5.4e+13	5.18e+13	3.94e+13	1.89e+13	3.53e+12

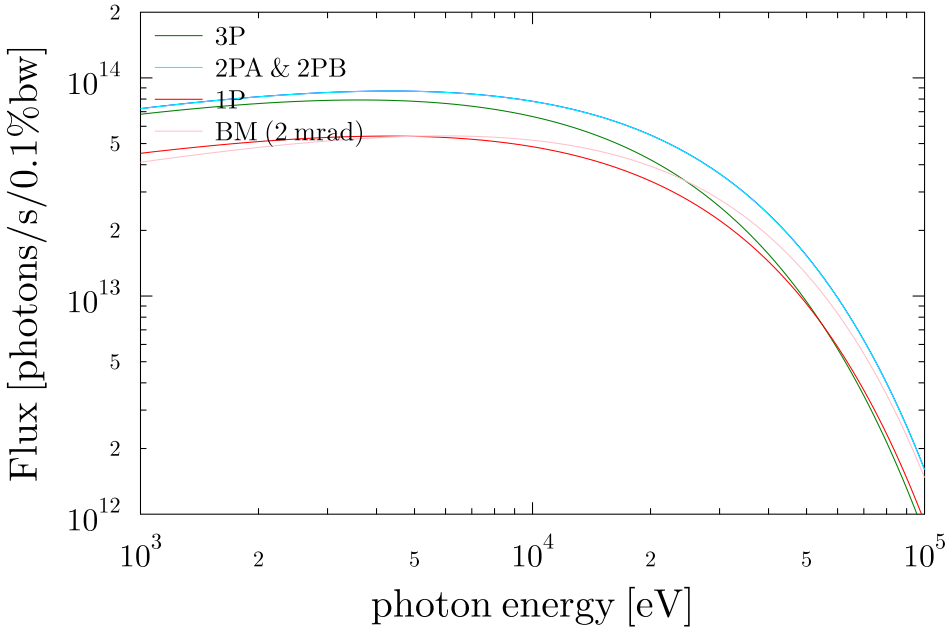

Figure 2: Calculated flux spectra produced by the ESRF-EBS short wigglers and the ESRF bending magnet.

4 Radiation geometry

In order to estimate the photon beam properties in the ideal case of *zero emittance* and no emission from the side BMs, a series of calculations have been preformed using the magnetic field in Fig. 2b. Results for all sources and focusing cases are summarized in Table 4. Full results are in a supplement document `short_wigglers_no_emittance.html`. The calculations are performed for photon energy $E = 5,\ 10,\ 20,\ 40,\ 80\ keV$.

Some comments about these results:

1. the horizontal divergence is $< 2\ mrad$. This is dictated by the maximum interval in transversal velocity which is approximately the maximum horizontal divergence $v_x/c \sim \theta_x$.

2. the vertical divergence is dictated by the photon emission angle and decreases with photon energy.

3. the ideal focus always presents tails due to the emission of different poles (for 2P and 3P) and the curved trajectory of the electrons (1P and BM). These tails are highly dependent on the geometry. These tails will be completetly smeared-out by the electron emittance (see later), because the FWHM values are usually very small. However, the tails for the 2PA and 2PB cases are higher than the half maximum, thus explaining the high values in these devices. In fact, the 2P case is the less favorable because of the two identical sources are at the limit of resolution, but their distance contribute to the width. In the other cases there is only one source (1P) or three (3P) but the central one dominates.

4. Even more pronounced, the toroidal 1:1 focusing shows small sizes for all cases, being the 2P the less favorable case as a result of the separation between the two poles emission. For 3P the different pole emissions are also separated but the most intense central pole dominates.

5. the focus of the short ID's is highly structured, because the emission is concentrated in the crests of the electron trajectory, and there is no emittance that smears out the source and the image. For this reason, the numeric values of FWHM in Table 4 may not be significative.

6. Technical consideration: the intensity profiles sometimes shows some numerical artifacts: a lack of intensity (holes) at given position and perhaps this intensity moved to another position. This is due to a problem in the interpolation and spline routines and will be solved, but for the moment just keep in mind that this is a calculation problem and has not physical sense.

Table 3: Photon beam divergence for the different short ID's for zero emittance. Negative values: failed to compute FWHM (it usually happens when size is $\leq 1\ \mu m$). Mirrors have no slope errors.

E	ID	H Div	V Div	H 1:1 ideal	V 1:1 ideal	H 1:1 toroid	V 1:1 toroid	H 3:1 ellip	V 3:1 ellip
eV		μrad	μrad	μm	μm	μm	μm	μm	μm
5	BM	1970	258	2.99	0.40	1.00	0.27	-1.00	-1.00
10	BM	1970	189	1.49	0.40	1.00	0.27	-1.00	-1.00
20	BM	1970	134	2.99	0.40	1.00	0.13	-1.00	-1.00
40	BM	1970	89	2.99	0.40	1.00	0.27	-1.00	-1.00
80	BM	1970	59	1.49	-1.00	1.00	-1.00	-1.00	-1.00
5	3Pcut	1462	216	4.48	0.60	1.00	2.39	-1.00	1.06
10	3Pcut	1402	156	4.48	0.40	1.00	1.86	-1.00	1.06
20	3Pcut	1373	109	2.99	0.40	1.00	1.33	-1.00	1.06
40	3Pcut	1253	82	2.99	-1.00	1.00	1.20	-1.00	1.59
80	3Pcut	1134	57	1.49	-1.00	1.00	0.93	-1.00	2.91
5	2PAcut	1582	226	7.46	4.78	45.85	3.06	19.87	2.65
10	2PAcut	1462	171	25.37	3.98	49.83	2.79	15.89	2.65
20	2PAcut	1402	119	41.79	2.59	50.83	2.39	15.89	2.65
40	2PAcut	1223	87	58.21	1.99	49.83	2.39	15.89	2.65
80	2PAcut	1044	54	56.72	1.19	50.83	2.52	15.89	2.65
5	2PBcut	1582	233	11.94	4.38	48.84	2.79	19.87	2.65
10	2PBcut	1462	169	34.33	3.18	51.83	2.66	15.89	2.65
20	2PBcut	1402	124	47.76	2.79	50.83	2.52	15.89	2.65
40	2PBcut	1223	84	56.72	1.99	50.83	2.79	15.89	2.65
80	2PBcut	1074	62	56.72	1.39	41.86	2.26	15.89	2.65
5	1Pcut	1820	233	1.49	0.80	1.00	0.40	-1.00	-1.00
10	1Pcut	716	161	1.49	0.40	1.00	-1.00	-1.00	-1.00
20	1Pcut	1343	114	2.99	0.20	1.00	0.27	-1.00	-1.00
40	1Pcut	328	82	2.99	-1.00	1.00	-1.00	-1.00	-1.00
80	1Pcut	776	57	1.49	-1.00	1.00	0.53	-1.00	-1.00
5	3P	1492	199	2.99	0.80	1.00	2.26	-1.00	-1.00
10	3P	1462	149	2.99	0.40	1.00	0.27	-1.00	-1.00
20	3P	1402	94	2.99	0.40	1.00	0.53	-1.00	-1.00
40	3P	1343	67	1.49	-1.00	1.00	0.13	-1.00	-1.00
80	3P	1134	54	1.49	-1.00	1.00	-1.00	-1.00	-1.00
5	2PA	1492	203	7.46	5.17	1.00	-1.00	1.99	-1.00
10	2PA	1462	139	29.85	3.38	2.99	0.80	-1.00	-1.00
20	2PA	1373	104	47.76	2.39	8.97	-1.00	-1.00	-1.00
40	2PA	1164	77	50.75	1.79	8.97	17.54	3.97	0.53
80	2PA	1074	59	55.22	1.19	9.97	19.14	3.97	1.06
5	2PB	1552	201	14.93	5.37	1.99	-1.00	3.97	-1.00
10	2PB	1492	161	35.82	3.58	7.97	0.40	3.97	-1.00
20	2PB	1313	114	50.75	2.79	6.98	1.73	1.99	-1.00
40	2PB	1253	72	52.24	1.99	8.97	5.71	3.97	0.53
80	2PB	1044	57	53.73	1.19	8.97	16.48	1.99	1.06
5	1P	5940	189	1.49	0.60	1.00	-1.00	-1.00	-1.00
10	1P	5970	136	2.99	0.40	1.00	-1.00	-1.00	-1.00
20	1P	3820	104	1.49	0.40	1.00	0.40	-1.00	-1.00
40	1P	1462	72	2.99	-1.00	1.00	0.13	-1.00	-1.00
80	1P	1402	59	1.49	-1.00	1.00	-1.00	-1.00	-1.00

5 Electron emittance

Emittance values for the EBS-ESRF lattice have been calculated using the AT package, with lattice file `S28CINJ.mat`, and emittance values of $\epsilon_x = 134\ pm$ and $\epsilon_z = 5\ pm$ and energy dispersion $\sigma_\delta = 10^{-3}$. The short ID center is at the lattice coordinate $s_w = 13.8379\ m$. Close to the short ID position, we find the DQ2C dipole upstream, and the quadrupole QF8 and dipole DQ1D downstream. Table 5 shows the position and values for these devices. Table 5 shows the Twiss parameters.

Table 4: Position of the center of the magnets referred to the cell's s coordinate and to the center of the ID (s_w).

AT index	magnet name	s (m)	$s - s_w$ (m)	length (m)	angle (rad)	Magnetic field (T)
63	DQ2C_2	13.3872	-0.4507	0.4	0.0078	0.393
	short ID	13.8379	0	~ 0.14		~ 0.8
68	QF8D	14.4302	0.5923	0.4840		
70	DQ1D	15.0342	1.1963	1.0280	0.0292	0.567

Table 5: Twiss parameters at center of devices

magnet name	s (m)	α_x	α_z	β_x (m)	β_z (m)	γ_x (m^{-1})	γ_z (m^{-1})	η_x η_x	η_z η_z
DQ2C_2	13.387	-0.584	1.364	0.605	4.421	2.216	0.647	0.012	0
short ID	13.838	-2.018	1.933	1.814	2.569	2.797	1.844	0.018	0
QF8D	14.430	2.616	-3.567	2.052	2.842	3.823	4.830	0.016	0
DQ1D	15.034	0.128	-0.098	0.546	6.057	1.862	0.167	0.006	0

At the ID center position the values of the α functions are large, meaning that the phase space ellipses at that position are tilted. The place where the phase ellipses are not tilted are called waist. At the waists, $\alpha = 0$ and the popular relation $\epsilon = \sigma\sigma'$ holds, where epsilon is the storage ring emittance (horizontal X, or vertical Z) and σ and σ' are related to the moments of the electron distribution: $\sigma_x =< xx >^{1/2}$, $\sigma'_x =< x'x' >^{1/2}$ (and similarly for y). Outside the waist this relation does not hold (it can be seen in Table 5 that for the ID center $\sigma_x\sigma'_x \simeq 587\ pm > \epsilon_x$). Moreover, the electron size and divergences are dictated not only by the Twiss parameters but also by the energy dispersion (functions η, η' and energy dispersion σ_δ):

$$\begin{aligned} < xx > &= \beta_x\epsilon_x + \eta_x^2\sigma_\delta^2 \\ < xx' > &= -\alpha_x\epsilon_x + \eta_x\eta'_x\sigma_\delta^2 \\ < x'x' > &= \gamma_x\epsilon_x + \eta_x'^2\sigma_\delta^2 \end{aligned} \tag{1}$$

and similarly for y.

Table 6 gives the position of the waists closer to the ID center, and the electron beam sizes.

Table 6: Values of α, β, σ and σ' for position of the waists closer to the ID center. The values at the ID center are also shown. Relative positions means from ID to waist.

location	waist $[m]$ (relative)	waist $[m]$ (absolute)	α	β m	σ μm	σ' μrad	$\sigma\sigma'$ pm
H upstream (β min)	-0.651	13.187	0.000	0.491	13.724	16.524	226.8
H (center)	0.000	13.838	-2.018	1.814	23.766	24.719	587.5
H downstream (β max)	0.327	14.165	-0.000	2.831	28.486	8.340	237.6
V upstream (β max)	-0.651	13.187	-0.000	4.700	4.848	1.031	5.0
V (center)	0.000	13.838	1.933	2.569	3.584	3.036	10.9
V downstream (β min)	0.286	14.123	-0.000	1.878	3.064	1.632	5.0

SHADOW include the effect of emittance. It asks for the values of the electron beam sizes and divergences **at the waist** and the distance from the waist. Then SHADOW calculates the values at any s point along the ID by propagating these values **in absence of magnetic field**. In a typical case where the ID is placed in a long straight section, one should give to SHADOW the parameters at the waist, as indicated in Table 5. However, in our case, the ID is very close to other magnets and the "real" waist positions are affected by these magnets, so the approximation of propagation in space absent of magnetic field is not valid.

In order to give parameters to SHADOW, we can find the positions of "fake" waists corresponding to the location of waist supposing that the ID is not surrounded by other magnets, but free space (no magnetic field). Fig. 3 shows the evolution of the cross terms $< xx' >$ and $< yy' >$ that are zero at the waists (also corrected by dispersion). From here, it can be found the "fake" horizontal waist at $s_w = -0.894\ m$ and "fake" vertical waist at $s_w = 1.048\ m$ from the ID center. Table 5 shows the values to be entered to SHADOW for the fake waists and a comparison of the "real" and "propagated" values at the center of the ID, showing a good agreement.

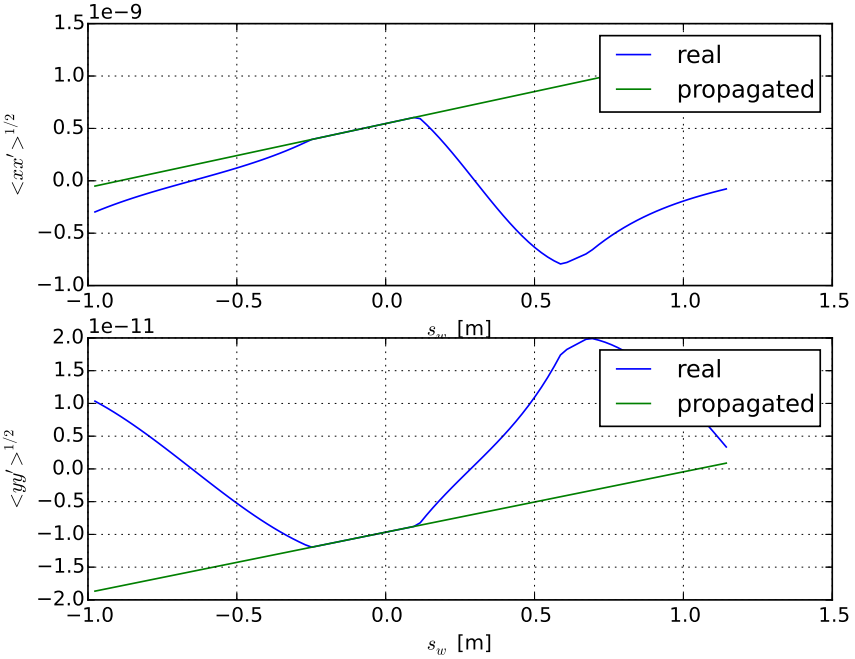

Figure 3: Evolution of $< xx >^{1/2}$ and $< yy' >^{1/2}$ around the ID center, in the EBS-ESRF lattice (blue) and in absence of sourrounding magnets (green).

Table 7: Values of the fake waists from where the propagation in absence of magnetic field gives correct values of electron beam moments at the ID center. Note that SHADOW input requires the distance from the waist to the ID center, thus the opposite of the values given here. Also, the emittance value to be entered in SHADOW are $\sigma\sigma'$, (because dispersion is not considered in SHADOW).

location	position $[m]$ (relative)	σ μm	σ' μrad	$\sigma\sigma'$ pm
H fake waist (downstream)	-0.894	8.757	24.72	216.47
H (center,propagated)	0	23.77	24.72	
H (center,real)	0	23.77	24.72	
V (center,real)	0	3.58	3.04	
V (center,propagated)	0	3.58	3.05	
V fake waist (upstream)	1.0480	1.647	3.036	5.00

Figure 4 shows a sampling of the electron horizontal phase space at the center of the ID.

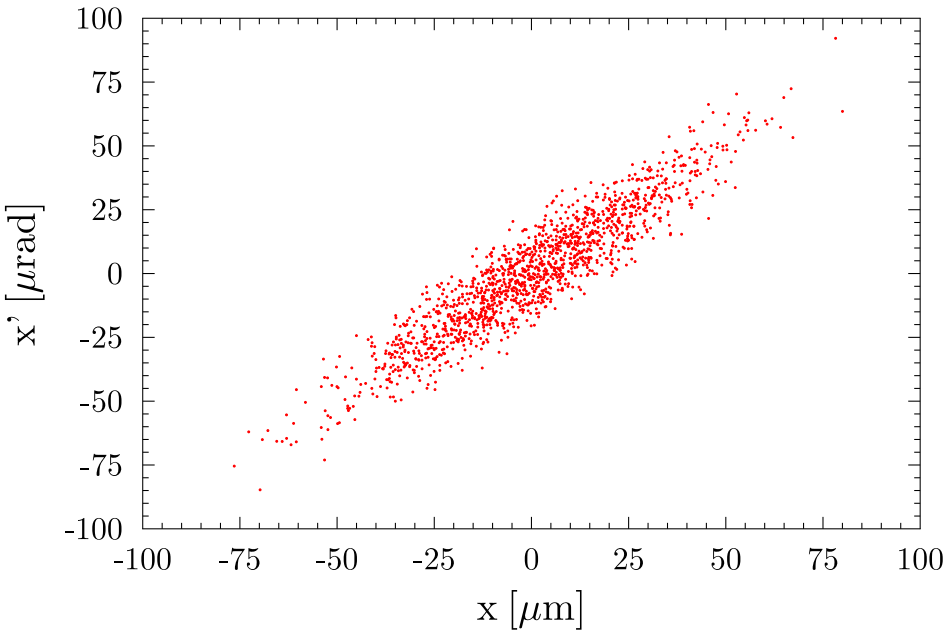

Figure 4: Sampling of the electron (x, x') phase space at the center of the ID.

For the ESRF-I bending magnet the parameters used are taken from the Orange book ($\sigma_x = 77.9\ \mu m, \sigma'_x = 110.9\ \mu rad, \sigma_z = 12.9\ \mu m, \sigma'_z = 0.5\ \mu rad$) giving therefore $\epsilon_x = \sigma_x \sigma'_x \sim 8600\ pm$ and $\epsilon_z = \sigma_z \sigma'_z \sim 6.45\ pm$. The distance to the waist has been taken to zero. The Table 5 shows the results for the wigglers with field in Fig. 2b, but including emittance. Full results are in the file: `short_wigglers_with_emittance.html`. Some conclusions can be extracted:

1. The divergence width values roughly vary as stated before (slightly reducing with photon energy in H and dictated by the photon emission in V)

2. The 3P H divergence presents a hole in the middle, more important for low photon energies, but still present at 80 keV. This was discussed in a previous document [1]. Also discussed there, the radiation presents ripples at the edges (not shown here, as these interference effects are not considered by SHADOW).

3. The ideal focusing gives for all short IDs much better smaller foci than the BM placed at ESRF-I, due to the much better emittance values for the new lattice. **Thus, source brillance increases a lot.** For example, at 20 keV the 1:1 ideally focused BM beam is 173x30μm^2 and for the 3P in the new lattice it is 51x9μm^2, therefore a gain factor $\sim$ 12. For the other cases, the gain goes from 6 to 15.

4. Ideal focus give too nice profiles (very well defined intensity distributions) much better than the profiles obtained by a more realistic 1:1 toroidal

focusing. Therefore, the ideal focus results results are usually not realistic for a typical beamline.

5. For the 3P the 1:1 focused beam with a toroid does not resolve the "three sources".

6. The toroidal forcused 2P beam neither resolves the two sources, if the beamline is well aligned tangent to the inflexion point of the electron beam trajectory. In the case that the beamline is aligned tangent to the electrons entering in the ID, the two sources are resolved. There is a highest sensibility of the beamline alignment for the 2P as compared with the other cases, due to the presence of two identical sources.

7. 3:1 focusing always present some structures due to the extended source. These structures are always present, even for the 1P and BM, so they are not originated by the multiple sources. The focal size for 2P is worse than 1P and 3P, because of the same intensity in the two sources which contribute to enlarge the width, as seen in the non-emittance case. However, the results are still very good (consider also that the 2P source is more intense than 1P and 3P).

Table 8: Photon beam divergence for the different short ID's for finite electron beam (with emittance). The toroidal and ellipsoidal mirrors have slope error of 0.85 μrad in the tangential direction (we used the profile number 26 of the DABAM database).

E	ID	H Div	V Div	H 1:1 ideal	V 1:1 ideal	H 1:1 toroid	V 1:1 toroid	H 3:1 ellip	V 3:1 ellip
eV		μrad	μrad	μm	μm	μm	μm	μm	μm
5	BM	1970	261	179.10	29.45	175.42	127.57	47.68	66.75
10	BM	1970	189	176.12	30.25	173.42	107.91	55.63	56.16
20	BM	1970	131	176.12	29.45	173.42	101.53	55.63	44.50
40	BM	1970	89	170.15	29.45	183.39	107.91	55.63	41.32
80	BM	1940	59	176.12	28.66	177.41	82.39	55.63	34.97
5	3Pcut	1432	218	56.72	7.96	55.81	74.95	19.87	30.73
10	3Pcut	1402	159	56.72	7.96	55.81	61.66	19.87	51.92
20	3Pcut	1373	114	53.73	7.96	57.81	57.41	19.87	30.73
40	3Pcut	1253	82	53.73	7.96	53.82	52.09	15.89	52.98
80	3Pcut	1134	59	53.73	7.96	51.83	48.90	15.89	50.86
5	2PAcut	1582	236	77.61	9.55	71.76	73.89	23.84	51.92
10	2PAcut	1492	179	77.61	9.55	75.75	61.66	23.84	30.73
20	2PAcut	1402	129	77.61	7.96	73.75	58.47	23.84	51.92
40	2PAcut	1253	87	71.64	7.96	75.75	55.28	23.84	52.98
80	2PAcut	1074	59	71.64	7.96	69.77	53.69	23.84	50.86
5	2PBcut	1582	238	77.61	9.55	71.76	70.17	23.84	32.85
10	2PBcut	1522	176	77.61	9.55	75.75	62.19	23.84	50.86
20	2PBcut	1402	124	71.64	7.96	75.75	59.53	23.84	52.98
40	2PBcut	1253	87	71.64	7.96	71.76	52.62	23.84	30.73
80	2PBcut	1074	59	71.64	7.96	69.77	52.09	23.84	52.98
5	1Pcut	2000	221	53.73	7.96	55.81	74.42	15.89	50.86
10	1Pcut	1820	171	50.75	7.96	51.83	68.57	15.89	32.85
20	1Pcut	1701	119	53.73	7.96	51.83	101.00	15.89	50.86
40	1Pcut	1492	84	53.73	7.96	55.81	55.28	15.89	49.80
80	1Pcut	1313	59	53.73	7.96	53.82	52.62	15.89	50.86
5	3P	1492	201	56.72	9.55	57.81	74.42	15.89	50.86
10	3P	1462	144	53.73	8.76	61.79	76.01	19.87	30.73
20	3P	1402	106	53.73	7.96	55.81	56.88	15.89	50.86
40	3P	1313	72	53.73	7.96	51.83	102.59	15.89	51.92
80	3P	1164	54	53.73	7.96	53.82	48.90	15.89	49.80
5	2PA	1552	199	80.60	9.55	45.85	140.86	15.89	57.22
10	2PA	1492	139	74.63	9.55	57.81	115.35	15.89	60.40
20	2PA	1373	106	71.64	9.55	49.83	108.44	15.89	54.04
40	2PA	1253	77	74.63	7.96	57.81	106.31	15.89	55.10
80	2PA	1074	57	71.64	7.96	53.82	45.18	15.89	52.98
5	2PB	1522	213	68.66	10.35	51.83	86.64	15.89	57.22
10	2PB	1462	149	68.66	8.76	55.81	118.54	15.89	22.25
20	2PB	1373	114	71.64	7.96	51.83	55.28	15.89	28.61
40	2PB	1223	82	71.64	7.96	49.83	97.81	19.87	51.92
80	2PB	1044	57	71.64	7.96	57.81	103.65	15.89	52.98
5	1P	5970	191	53.73	7.96	49.83	120.66	11.92	46.62
10	1P	5970	146	56.72	7.96	51.83	100.47	15.89	26.49
20	1P	3850	101	50.75	7.96	49.83	111.10	15.89	51.92
40	1P	1582	77	53.73	7.96	51.83	56.88	15.89	47.68
80	1P	1373	54	50.75	7.96	53.82	49.97	15.89	49.80

6 Overlapping radiation by the magnets in the neighbour

For studing the overlapping effect of the side bending magnet, it is useful starting to study the effect of these BMs withouth insertion device. For that a case labelled "0P" (zero poles) is calculated for all cases studied here. Results are in the file: `short_wigglers_with_emittance.html`. Looking at the intensity vesus divergence, it can be shown that for high photon energies the radiation from the downtream BM (DQ1D) dominates, because its high magnetic field. This is not the case for low energies (e.g., at 5 keV), where the intensity of the emission from both BMs is similar. Moreover, at low energies the gap left between the radiation of the two BMs is very small, thus a background will be unavoidable. Ah high energies, the separation gap increases, helping to isolate the ID radiation and reducing the background. In general, the size of the focused beam including theirside BMs is similr to the size withouth BMs (compare in Table8 the values without BMs, labelled with "cut" with those with BMs). It can be concluded that a background from the side BMs is unavoidable, its effect is more important at low photon energies, and does not affect to the focal beam sizes. Because these size beams are not focused at the same point than the central ID, their effect is less important when using focalization. However, each particular beamline should be studied in more detail.

References

[1] Sanchez del Rio, Manuel . Simulations of radiation from a 3-pole wiggler. Comparison between the ESRF and the APS upgrade projects. *Unpublished*, 2014.